https://doi.org/10.56801/MME985

Dynamic Analyses of Two-Dimensional Functionally Graded Timoshenko Beam using Finite element Method

Dhyai Hassan jawad Aljashaami[1], Mohammed A Al-Shujairi[2], Ameen M. Al Juboori[3], Salwan Obaid Waheed Khafaji[2], Mohammed Jawad Aubad[4]

[1]*University of Babylon, College of Engineering/ Al-Musayyab, Department of Automobiles Engineering, Iraq.*
[2]*University of Babylon, College of Engineering, Department of Mechanical Engineering, Iraq.*
[3]*Al-Mustaqbal University Collage, Biomedical Engineering Department, Babylon, Iraq.*
[4]*University of Babylon, College of Engineering, Department of Mechanical Engineering, Iraq, eng.mohammed.j.tarfa@uobabylon.edu.iq*

Received: 15-02-2023
Accepted: 31-03-2023

Abstract: In this work, dynamic analyses of a functionally graded beam are presented. The governing equations of the beam is found based on the displacement field defined by Timoshenko beam theory, then solved by using finite element method based on Hamilton's principle. The beam is assumed to be free-clambed boundary condition (F-C). The PL index is used for describing the distribution of the beam properties in both transverse and longitudinal directions. A parametric study is accomplished to investigate effect of several parameters on the natural frequency, mode shapes and transient response of the beam., such as the PL indexes (nx and nz) for x and z axis, respectively, and the elasticity modulus ratio (Eratio). To valid the present results and current mathematical formulation, some of the findings are compared with another research. A good agreement is noticed. It is noted that the response of the beam is more sensitive to the variations of the PI in the longitudinal axes than that corresponding in the transverse one. For specific design requirements, the dynamic response of the beam can be adjusted by chose a proposal indexes and modulus ratios.

Keywords: elasticity modulus ratio (Eratio); free-clambed boundary.

1. Introduction

Currently, one of the important requirements for improving structural performance in industrial engineering is using materials that offer continuously varying properties along different coordinates. The heterogeneous properties of materials can be existed in the functionally graded (FG) materials by mixing metal and ceramic with a variation the properties along transverse, axial or width directions [1; 2]. The basic structure of a FG material (FGM) depends on the different thermal stress concentrations of the constituent materials, where the ceramic and metal show better resistance of the thermal and mechanical stresses, respectively [3]. Due to these properties and advantages, the FG material is superior for several high-tech industries for real life applications, such as nuclear, automotive, biomedical, aerospace, and

*Corresponding authors: Mohammed Jawad Aubad, eng.mohammed.j.tarfa@uobabylon.edu.iq

other applications [4; 5]. For example. Karamanli [6] illustrated the bending analysis of laminated beams with two-directional FG material based on different theories (Euler-Bernoulli (EB), First order shear deformation (FOSD) and Reddy–Bickford). Several parameters were studied, such as aspect ratio, BCs, PL index, and sandwich structures. Karamanli [7] studied the modal analysis of a bi-directional FG beam using the displacement field described by the higher-order shear deformation theory (HOSDT) for various BCs. The material properties (MP) of FG beam varied in two directions. Effect of power indices (PIs), BCs, and aspect ratios on the free vibration of FG beam structure were presented. Wang et, al. [8] used the analytical solution to study the modal analysis characteristics of 2-D FG beam with EB beam theory for various BCs. The MP were varied smoothly in the length and thickness according to power law (PL) distribution and an exponential gradation, respectively. Simsek [9] investigated the buckling analysis of an FG beam in two dimensions with various BCs based on the Timoshenko beam theory (TBT) and EB beam theory. He used Ritz method to find the critical bucking load. Karamanli et, al. [10] studied the flexural behaviors of two-dimension FG micro-beam by FEM and parabolic shear deformation theory of the beam based with various BCs. The MP varied smoothly through x-axis and z-axis of the beam based on the PL distribution. Karamanli [11] presented the electrostatic analysis of beam made of bi-directional FG material based on the various beam theories with different BCs. Simsek [12] investigated vibration characteristics of 2D-FG beam based on the FOSD theory and EBT under effect of as moving load. Equations of motions (EoMs) were derived based on Lagrange method for various BCs. Effect of degradation in beam materials, BCs, and beam sectional ratio on the dynamic behavior of bi-directional FG beams were investigated. Trinh et, al. [13] estimated the modal analysis of FG beams in 2-D according to the modified theory of the couple stress with a quasi-3D theory. Hamilton's principle (HP) was used for deriving EoMs. The MP were assumed to change exponentially through z-axis and x-axis of FG micro-beam. Deng Hao et al [14] applied Lagrange equation to establish the differential equations of the two-dimensional FG beam based on TBT under different BCs. EOMs with corresponding BCs were derived based HP. MP were varied gradually in the longitudinal and transverse directions, respectively. Tanga et al. [15] computed the hygro-thermal dynamic of the two-dimensional FG beam with nonlinear behavior based on the EBT for different BCs. They used von Kármán nonlinearity and HP for derivation the governing equations. Karamanli [16] discussed analysis of bending of sandwich bi-directional FG beam according to the 3-D shear deformation theory for different BCs. Nejad et, al [17] illustrated the analysis of the beam buckling of size-dependent 2-D FG beam based on the EBT with Eringen's nonlocal theory. They used the potential energy principle for deriving the EoM. Yang et, al. [18] investigated buckling, free vibration, and static analyses of 2D-FG beam with von Kármán principle for the geometrical nonlinearity. Li et, al. [19] investigated the static analysis of 2-D nonlinear FG beam according to CBT in conjunction with the minimum potential energy principle. EoMs and the related various BCs were solved by using the method of the generalized differential quadrature. Nejad et, al. [17] examined the bending analysis of size-dependent two-directional FG nano-beam according to the EBT along with the Eringen's nonlocal theory. Nejad et, al. [20] reported the modal analysis of bi-directional FG small scale beam with the CBT and the Eringen's-nonlocal theory. Based on the literature survey presented above, very few studies showed the effect of material variation in two dimensions in FG beams. Moreover, literatures showed no similar work on the transient response of a bi-directional FG beam by using the finite element (FE) method in conjunction with TBT where the PI vary instantaneously. In this study, the modal and transient analyses of a 2D-FG beam based on TBT with the FEM has been investigated. The HP is used for deriving the governing equations. PL index of the FGM for distribution the properties in two directions (x and z) is used. Free vibration results are illustrated and compared with another work to check the modeling accuracy. A reasonable convergence is noticed in the results. Finally, the effect of modulus ratio and PI on the free vibration characteristics and transient dynamic response has been studied.

2. Mathematical Modeling

2.1 Material Properties

Figure 1 shows an FGM beam of dimensions L, b, and h for length, width, and height. The properties vary from left to right and bottom to top. The FG beam consists of two fundamental materials. The effective MPs are considered to be distributed in the transverse and longitudinal directions (z and x) based on the PL as:

$$P(x,z)=(P_t-P_b)\left(\frac{z}{h}+\frac{1}{2}\right)^{n_z}\left(1-\frac{x}{L}\right)^{n_x}+P_b \tag{1}$$

In equation (1), the term $P(x,z)$ represents the effective value of the selective MP, including Poisson ratios, mass density, shear modulus, and Young's modulus. The sub-indices b and t are symbols for indicating the bottom and top of the beam, respectively. n_x and n_z are positive PL index, express the constituent materials distribution as shown in Figure 2.

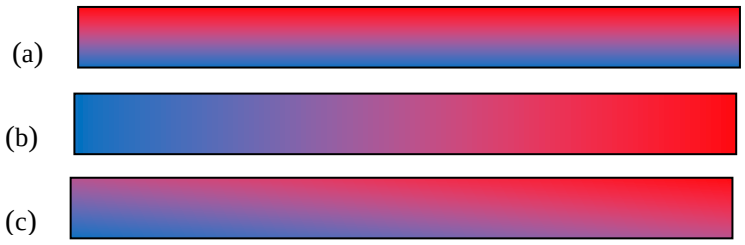

Figure 1. *Geometry of FG Timoshenko beams through: (a) a thickness, (b) an axially and (c) a bi-directional*

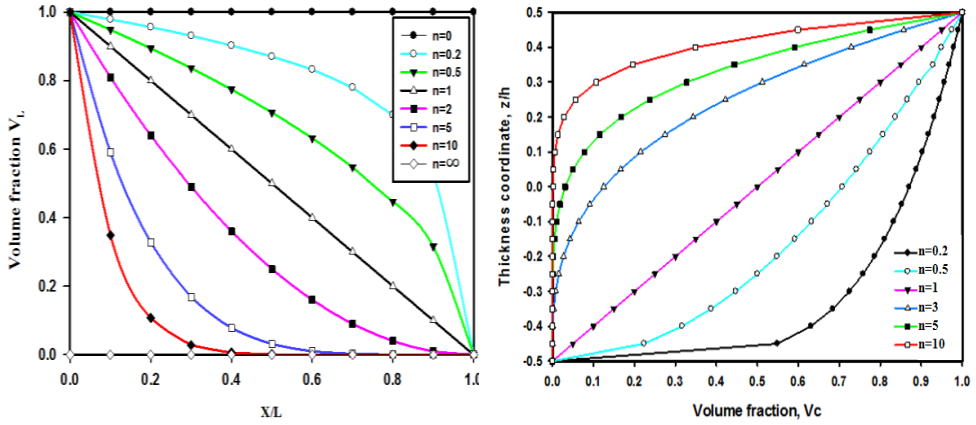

Figure 2. *Variation of the volume fraction of the ceramic constituent along (a) the thickness and (b) the length*

2.2 The Governing Equation of Motion

The displacement field for the TBT [21], for the beam shown in Figure 3, can be given by,

$$u(x,z)=-z\theta(x) \tag{2a}$$

$$w(x,z) = w(x) \tag{2b}$$

where $w(x)$ and $\theta(x)$ are the rotation and transverse displacement respectively. The strain and stress are given in terms of displacement by,

$$\varepsilon_x = \frac{\partial u}{\partial x} = -z\frac{\partial \theta}{\partial x} \tag{3a}$$

$$\gamma_{zx} = \frac{\partial w}{\partial x} - \theta \tag{3b}$$

$$\sigma_x = E(x,z)\,\varepsilon_{xx} \tag{3c}$$

$$\tau_{xz} = k\,G(x,z)\,\gamma_{xz} \tag{3d}$$

where, k is the surface factor for correction. The Poisson's ratio hold constant in this work. Furthermore, strain energy of the 2-D FG beam involves two parts, one of them results from FG material, and the other from the material homogeneity assumption with the constituent. The strain energy resulted from equation (3) and equation (4) for FG beam can be written as:

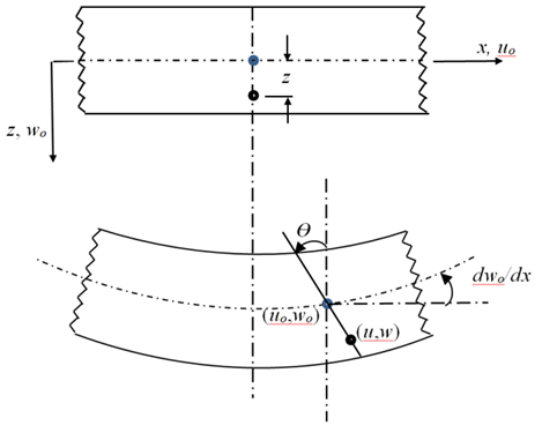

Figure 3. *Deformation of Timoshenko beam*

$$U_{S.E} = \frac{1}{2}\int_A\int_0^L \left(\sigma_x\varepsilon_x + \tau_{xz}\gamma_{xz}\right) dA\,dx \tag{5}$$

This Equation can be modified by some mathematical manipulation as,

$$U_{S.E} = \frac{1}{2}\int_A\int_0^L \left(E(x,z)\,{\varepsilon_{xx}}^2 + k\,G(x,z)\,{\gamma_{xz}}^2\right) dA\,dx$$

$$U_{S.E} = \frac{1}{2}\int_A\int_0^L \left(E(x,z)\,z^2\left(\frac{\partial\theta}{\partial x}\right)^2 + k\,G(x,z)\left(\frac{\partial w}{\partial x} - \theta\right)^2\right) dA\,dx \tag{6}$$

$$U_{S.E} = \frac{1}{2}\int_0^L \left[\left(D_{bending}\left(1-\frac{x}{L}\right)^{n_x} + E_b I\right)\left(\frac{\partial\theta}{\partial x}\right)^2 + k\left(D_{shear}\left(1-\frac{x}{L}\right)^{n_x} + G_b A\right)\right] dx$$

where $D_{bending}$ and D_{shear} are the bending and shear rigidly, respectively, and given by

$$D_{bending} = \int_A z^2 E(z)\,dA \quad \text{and} \quad D_{shear} = \int_A G(z)\,dA \text{, respectively.}$$

where $E(z)$ and $G(z)$ are the modulus of elasticity and shear modulus in term of z- direction only. The kinetic energy is then given as,

$$\begin{aligned} K.E &= \frac{1}{2}\int_A\int_0^L \rho(x,z)\left(\left(\frac{\partial u}{\partial t}\right)^2 + \left(\frac{\partial w}{\partial t}\right)^2\right) dA\,dx \\ K.E &= \frac{1}{2}\int_A\int_0^L \rho(x,z)\left(z^2\left(\frac{\partial \theta}{\partial t}\right)^2 + \left(\frac{\partial w}{\partial t}\right)^2\right) dA\,dx \end{aligned} \tag{7}$$

which can be given in terms of inertia as,

$$K.E = \frac{1}{2}\int_0^L \left(I_1\left(\frac{\partial \theta}{\partial t}\right)^2 + I_2\left(\frac{\partial w}{\partial t}\right)^2\right) dx \tag{8}$$

where $I_1, I_2 = \int_A \rho(z)\left(z^2, 1\right) dA$

2.3 Finite Element Formulation

The beam is discretized by n beam elements. Two nodes element with two DoF at each node was used in this work. The total degrees of the freedom can be explained in Equation 9 as,

$$\vec{q} = \begin{bmatrix} w_1 & \theta_1 & w_2 & \theta_2 \end{bmatrix}^T \tag{9}$$

where w_i, θ_i are the transvers and rotational displacements at each node, respectively. The shape functions of the element for transvers and rotation for their nodal displacements can be given by,

$$w = \left\{N_w\right\}^T q, \theta = \left\{N_G\right\}^T q \tag{10}$$

where $\left\{N_w\right\}$ and $\left\{N_G\right\}$ are shape functions vectors for w and θ, respectively [2].

$$\left.\begin{aligned} N_{w1} &= \left(1/(1+\phi)\right)\left(2z^3 - 3z^2 - z\phi + (1+\phi)\right); \\ N_{w2} &= \left(L/(1+\phi)\right)\left(z^3 - \left(2 + (\phi/2)\right)z^2 + z\left(1 + (\phi/2)\right)\right); \\ N_{w3} &= -\left(1/(1+\phi)\right)\left(2z^3 - 3z^2 - z\phi\right); \\ N_{w4} &= \left(L/(1+\phi)\right)\left(z^3 - \left(1 - (\phi/2)\right)z^2 + z\,\phi/2\right); \end{aligned}\right\} \tag{11}$$

$$\left.\begin{aligned} N_{G1} &= \left(6/(L+\phi L)\right)\left(z^2 - z\right); \\ N_{G2} &= \left(1/(1+\phi)\right)\left(3z^2 - z(4+\phi) + (1+\phi)\right); \\ N_{G3} &= -\left(6/(L+\phi L)\right)\left(z^2 - z\right); \\ N_{G4} &= \left(1/(1+\phi)\right)\left(3z^2 - z(2-\phi)\right); \end{aligned}\right\} \tag{12}$$

where,

$$z = x/L \; and \; \phi = \frac{12 D_{bending}}{k \, L^2 D_{shear}}$$

2.4 Equation of Motion of the Entire System

The dynamic equation of motion for the damped structural is usually given by,

$$M\ddot{q} + C\dot{q} + Kq = F \tag{13}$$

The mass matrix M, damping matrix C, and stiffness matrix K are (n+1) by (n+1) in dimensions. F is the generalized external force vector at time (t) of the system. After substitution the shape functions for Equations (11 and 12) into Equation (5) and Equation (7), the total strain and kinetic energies for all element is obtained in the form,

$$U_{S.E} = \frac{1}{2} \sum_{i}^{n_{element}} q^T K \, q = \frac{1}{2} \sum_{i}^{n_{element}} q^T \left(K_b + K_s \right) q \tag{14}$$

where $n_{element}$ is the elements number, it is consisting from bending stiffness (K_b) and shear stiffness (K_s). These stiffness can be expressed as,

$$K_b = \int_0^L \left\{ N_G' \right\}^T D_{bending} \left\{ N_G' \right\} dx \tag{15}$$

$$K_s = \int_0^L \left\{ N_w' - N_G \right\}^T k \, D_{bending} \left\{ N_w' - N_G \right\} dx \tag{16}$$

The kinetic energy can be formed as,

$$K.E = \frac{1}{2} \sum_{i}^{n_{element}} \dot{q}^T M \, \dot{q} = \frac{1}{2} \sum_{i}^{n_{element}} \dot{q}^T \left(M_G + M_w \right) \dot{q} \tag{17}$$

where,

$$M_G = \int_0^L \left\{ N_G \right\}^T I_1 \left\{ N_G \right\} dx \tag{18}$$

$$M_G = \int_0^L \left\{ N_G \right\}^T I_1 \left\{ N_G \right\} dx \tag{19}$$

Usually, the stiffness matrix, mass matrix and damping matrix are given as:

$$[K]=\left[K_b\right]+\left[K_s\right]=\begin{bmatrix} k_{11b} & k_{12b} & k_{13b} & k_{14b} \\ k_{21b} & k_{22b} & k_{23b} & k_{24b} \\ k_{31b} & k_{32b} & k_{33b} & k_{34b} \\ k_{41b} & k_{42b} & k_{43b} & k_{44b} \end{bmatrix}+\begin{bmatrix} k_{11s} & k_{12s} & k_{13s} & k_{14s} \\ k_{21s} & k_{22s} & k_{23s} & k_{24s} \\ k_{31s} & k_{32s} & k_{33s} & k_{34s} \\ k_{41s} & k_{42s} & k_{43s} & k_{44s} \end{bmatrix} \tag{20}$$

where,

$$k_{11b}=\frac{12D_b}{L^3\left(R+1\right)^2} \qquad k_{11s}=\frac{k\,D_s\,R^2}{L\left(R+1\right)^2}$$

$$k_{12b}=k_{21b}=\frac{6D_b}{L^2\left(R+1\right)^2} \qquad k_{12s}=k_{21s}=\frac{k\,D_s\,R^2}{2\left(R+1\right)^2}$$

$$k_{13b}=k_{31b}=\frac{-12D_b}{L^3\left(R+1\right)^2} \qquad k_{13s}=k_{31s}=-\frac{k\,D_s\,R^2}{L\left(R+1\right)^2}$$

$$k_{14b}=k_{41b}=\frac{6D_b}{L^2\left(R+1\right)^2} \qquad k_{14s}=k_{41s}=-\frac{k\,D_s\,R^2}{2\left(R+1\right)^2}$$

$$k_{22b}=\left(\frac{D_b}{L}+\frac{3D_s}{L\left(R+1\right)^2}\right) \qquad k_{22s}=\frac{k\,D_s\,R^2L}{4\left(R+1\right)^2}$$

$$k_{23b}=k_{32b}=\frac{-6D_b}{L^2\left(R+1\right)^2} \qquad k_{23s}=k_{32s}=-\frac{k\,D_s\,R^2}{2\left(R+1\right)^2}$$

$$k_{24b}=k_{42b}=\frac{-D_b}{L}+\frac{3D_b}{L\left(R+1\right)^2} \qquad k_{24s}=k_{42s}=\frac{k\,D_s\,R^2\,L}{4\left(R+1\right)^2}$$

$$k_{33b}=\frac{12D_b}{L^3\left(R+1\right)^2} \qquad k_{33s}=\frac{k\,D_s\,R^2}{L\left(R+1\right)^2}$$

$$k_{34b}=k_{43b}=\frac{-6D_b}{L^2\left(R+1\right)^2} \qquad k_{34s}=k_{43s}=-\frac{k\,D_s\,R^2}{2\left(R+1\right)^2}$$

$$k_{44b}=\frac{D_b}{L}+\frac{3D_b}{L\left(R+1\right)^2} \qquad k_{44s}=\frac{k\,D_s\,R^2\,L}{4\left(R+1\right)^2}$$

While the mass matrix can be given as,

$$\left[m\right]=\left[M_G\right]+\left[M_w\right]=\begin{bmatrix} m_{11G} & m_{12G} & m_{13G} & m_{14G} \\ m_{21G} & m_{22G} & m_{23G} & m_{24G} \\ m_{31G} & m_{32G} & m_{33G} & m_{34G} \\ m_{41G} & m_{42G} & m_{43G} & m_{44G} \end{bmatrix}+\begin{bmatrix} m_{11w} & m_{12w} & m_{13w} & m_{14w} \\ m_{21w} & m_{22w} & m_{23w} & m_{24w} \\ m_{31w} & m_{32w} & m_{33w} & m_{34w} \\ m_{41w} & m_{42w} & m_{43w} & m_{44w} \end{bmatrix} \tag{21}$$

where,

$$m_{11G}=\frac{I_{11}L\left(70R^2+147R+78\right)}{210\left(R+1\right)^2} \qquad m_{11w}=\frac{6I_{22}}{5L\left(R+1\right)^2}$$

$$m_{12G}=m_{21G}=\frac{I_{11}L^2\left(35R^2+77R+44\right)}{840\left(R+1\right)^2} \qquad m_{12w}=m_{21w}=-\frac{I_{22}\left(5R-1\right)}{10\left(R+1\right)^2}$$

$$m_{13G}=m_{31G}=\frac{I_{11}L^2\left(35R^2+63R+27\right)}{210\left(R+1\right)^2} \qquad m_{13w}=m_{31w}=-\frac{6I_{22}}{5L\left(R+1\right)^2}$$

$$m_{14G}=m_{41G}=-\frac{I_{11}L^2\left(35R^2+63R+26\right)}{840\left(R+1\right)^2} \qquad m_{14w}=m_{41w}=-\frac{I_{22}\left(5R-1\right)}{10\left(R+1\right)^2}$$

$$m_{22G}=\frac{I_{11}L^3}{840\left(R+1\right)^2}+\frac{I_{11}L^3}{120} \qquad m_{22w}=\frac{I_{22}L\left(-5R^2+5R+1\right)}{30\left(R+1\right)^2}$$

$$m_{23G}=m_{32G}=\frac{I_{11}L^2\left(35R^2+63R+26\right)}{840\left(R+1\right)^2} \qquad m_{23w}=m_{32w}=\frac{I_{22}\left(5R-1\right)}{10\left(R+1\right)^2}$$

$$m_{24G}=m_{42G}=\frac{I_{11}L^3}{840\left(R+1\right)^2}-\frac{I_{11}L^3}{120} \qquad m_{24w}=m_{42w}=-\frac{I_{22}L\left(-5R^2+5R+1\right)}{30\left(R+1\right)^2}$$

$$m_{33G}=\frac{I_{11}L\left(70R^2+147R+78\right)}{210\left(R+1\right)^2} \qquad m_{33w}=\frac{6I_{22}}{5L\left(R+1\right)^2}$$

$$m_{34G}=m_{43G}=-\frac{I_{11}L^2\left(35R^2+77R+44\right)}{840\left(R+1\right)^2} \qquad m_{34w}=m_{43w}=\frac{I_{22}\left(5R-1\right)}{10\left(R+1\right)^2}$$

$$m_{44G}=\frac{I_{11}L^3}{120}+\frac{I_{11}L^3}{840\left(R+1\right)^2} \qquad m_{44w}=\frac{I_{22}L\left(10R^2+5R+4\right)}{30\left(R+1\right)^2}$$

where L is the element length,

$$R=\frac{12D_b}{k\,D_s\,L^2},\ D_b=\int_A z^2E\left(z\right)dA,\ D_s=\int_A G\left(z\right)dA,\ \ I_1=\int_A \rho\left(z\right)dA, I_2=\int_A z^2\rho\left(z\right)dA, and\ \ dA=b\,dz$$

The damping matrix [C] is Rayleigh-type damping [22] so that,

$$\left[C\right]=\alpha\left[M\right]+\beta\left[K\right] \tag{22}$$

The parameters α and β are proportionality factors which depend on the material types.

On the other hand, for free vibration, the equation of motion in eq. (13) become:

$$\left[M\right]\left\{\ddot{q}\right\}+\left[K\right]\left\{q\right\}=\left\{0\right\} \tag{23}$$

where,

$$\left\{q_i\right\}=\left\{\varphi_i\right\}\sin\omega_i t;\quad i=1,2,.....,k \tag{24}$$

After some mathematical presses, eq. (23) become:

$$\left(\left[K\right]-\omega_i^2\left[M\right]\right)\left\{\varphi_i\right\}=\left\{0\right\} \tag{25}$$

3. Results and Discussion

3.1 Results Verifications

In order to validate the mathematical modelling and the FE simulation, the dimensionless natural frequencies ($\lambda_1=\left(\omega_1 L^2/h\right)\sqrt{\left(\rho_m/E_m\right)}$) of two dimensional FG beam with clamped-free BC and TBT are compared with some results appeared in Ref. [12]. These values are listed in Table (1). A good agreement is noticed between the present work and Ref.[12].

Table 1 *Dimensionless fundamental frequency,* $\lambda_1=\left(\omega_1 L^2/h\right)\sqrt{\left(\rho_m/E_m\right)}$ *of bi-directional FG beam with CF boundary condition.*

		n_z					
n_x		0	0.2	0.4	0.6	0.8	1
0	**Ref. (12)**	**0.9844**	**0.9832**	**0.9796**	**0.9735**	**0.9661**	**0.9576**
	Present	0.9821	0.9811	0.9802	0.9726	0.9678	0.9569
0.2	**Ref. (12)**	**0.9271**	**0.9246**	**0.9222**	**0.9173**	**0.9100**	**0.9013**
	Present	0.9269	0.9251	0.9230	0.9175	0.9098	0.9009
0.4	**Ref. (12)**	**0.8709**	**0.8697**	**0.8673**	**0.8624**	**0.8564**	**0.8486**
	Present	0.8712	0.8691	0.8671	0.8616	0.8561	0.8489
0.6	**Ref. (12)**	**0.8193**	**0.8173**	**0.8154**	**0.8115**	**0.8037**	**0.7978**
	Present	0.8189	0.8169	0.8151	0.8112	0.8031	0.7971
0.8	**Ref. (12)**	**0.7685**	**0.7685**	**0.7666**	**0.7607**	**0.7548**	**0.7490**
	Present	0.7681	0.7679	0.7660	0.7601	0.7544	0.7485
1	**Ref. (12)**	**0.7216**	**0.7216**	**0.7177**	**0.7138**	**0.7099**	**0.7021**
	Present	0.7211	0.7210	0.7170	0.7132	0.7092	0.7019

3.2 Free Vibration Modes

As mentioned previously, the beam in current study is made from steel and alumina. Table 2 presents the properties of these materials.

Table 2 *Material properties of the functionally graded material beam constituent* Ref. [21]

Material	Property		
	Young Modulus (E)	Density (ρ)	Poisson's ratio (ν)
Steel	210 GPa	7800 kg/m^3	0.3
Alumina (Al_2O_3)	390 GPa	3960 kg/m^3	0.3

The first three modes of the FGM Timoshenko beam for cantilever BC at different PL indices on both directions are presented in Figures (4-6). The results are excluded at h/L=0.1. The correction factor is assumed to be 5/6.

It is noted that variations of the law index show no changes in the mode shapes of the cantilever FGM beam. However, the amplitudes are slightly different due to variation of the material distribution throughout the beam domain.

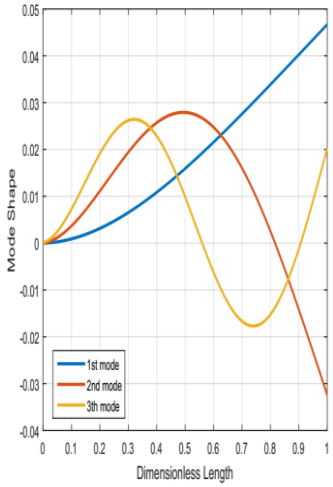

Figure 4. *The first three modes of cantilever FGMT beam with law power (nx=0, nz=0)*

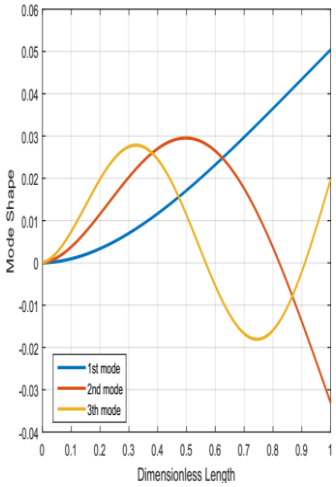

Figure 5. *The first three modes of cantilever FGMT beam with law power (nx=1, nz=1)*

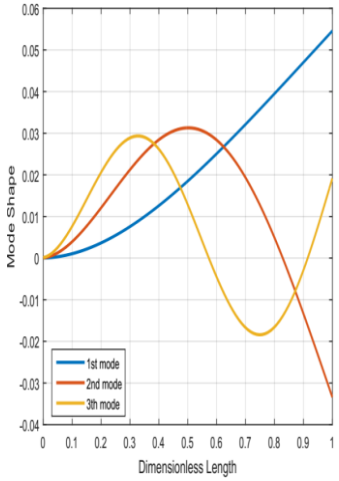

Figure 6. *The first three modes of cantilever FGMT beam with law power (nx=4, nz=4)*

Figure 7 and figure 8 show the three mode shapes individually at different values of PI in both directions of the beam. No changes in overall behavior of the mode shapes are noticed. However, insignificant changes in their values are noticed. Values decreases with increasing the PI in the thickness direction due to the domination of the Alumina which is stiffer than steel.

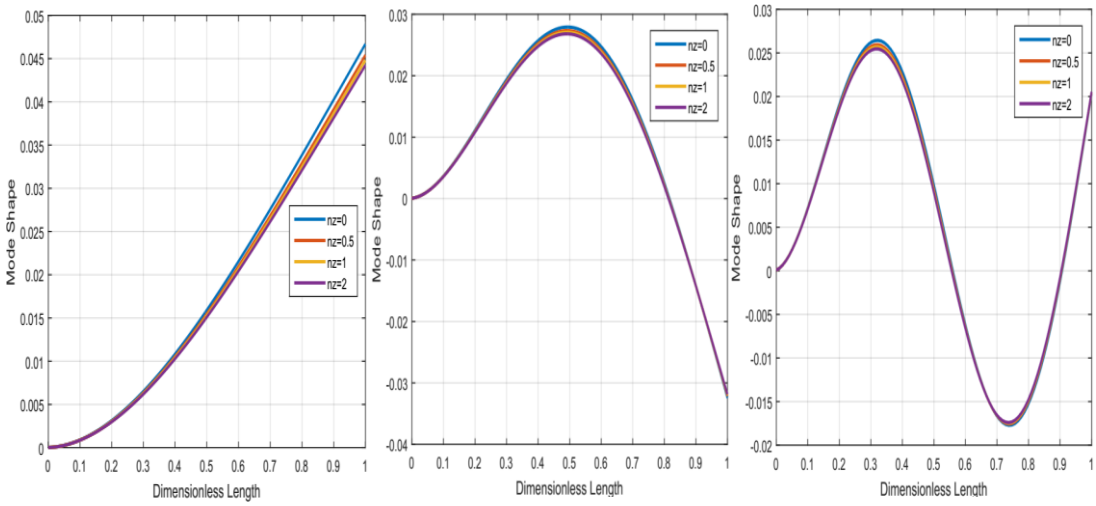

Figure 7. *The first three modes of cantilever FGMT beam with law power index (nx=0), b=.05m,h=0.005m, h/l=0.1*

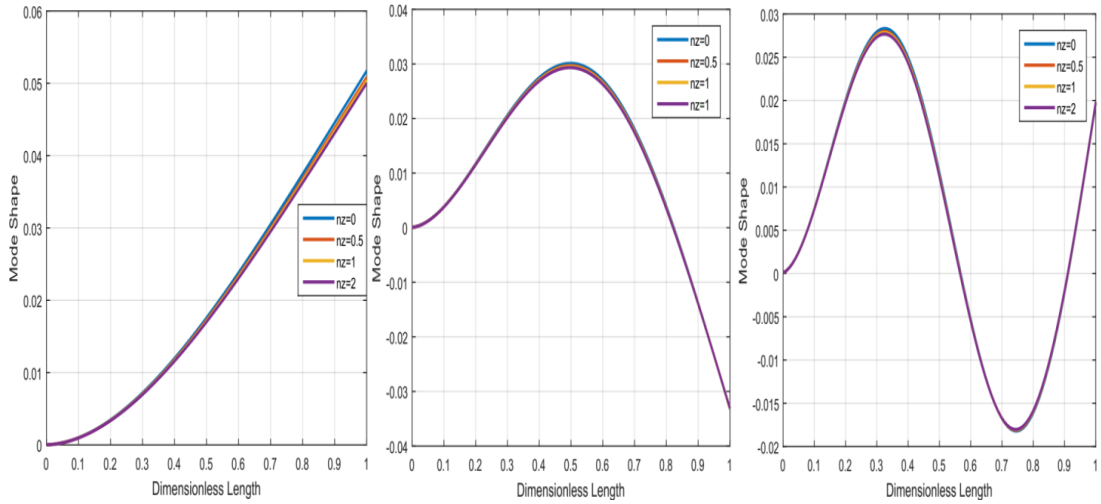

Figure 8. *The first three modes of cantilever FGMT beam with law power index (nx=1), b=.05m, h=0.005m, h/l=0.1*

3.3 Transient Analysis

In this section, the transient response of the FGM beam is illustrated for different values of gradient index (nx, nz) and moduli ratios. For more convenient, the effects will be presented in separate sections.

3.4 Effect of Power Law Index

Figures 9-14 shows the transient response for different PL indices in both directions of the cantilever beam under the effect of step input force of -10N. As noticed from Figure 9 and Figure 10, the transient response increases as the indices increase in both directions. Furthermore, amplitude and frequency slightly decreases as the indices increase because of the

domination of the steel material that is more flexible (lower stiffness) compared to the alumina. The steady state time and dynamic response are linearly proportional to PI. The domination of the Alumina (Al2O3) provides a stiffer beam, higher damping characteristics, and higher damped frequencies as shown in Figure 10. Similar behaviour is noticed in Figure 11 and Figure 12, where the transient responses are illustrated for different PL indices in both directions (not equal).. The trend of increasing the amplitude is the same so that the beam of the higher indices shows the higher transient response independent on which one of the indices are bigger. The same conclusion is valid for the steady state time response.

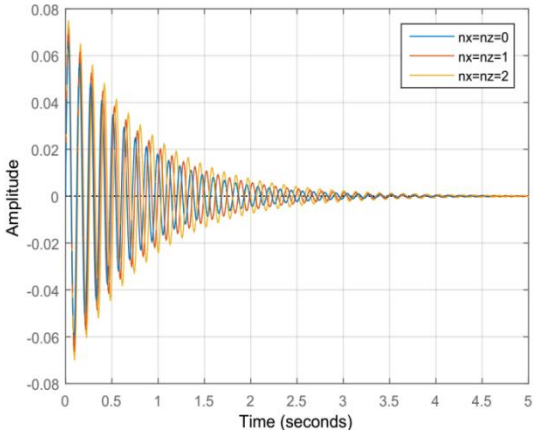

Figure 9. *Transient response of cantilever FGM beam with variable value of law power index*

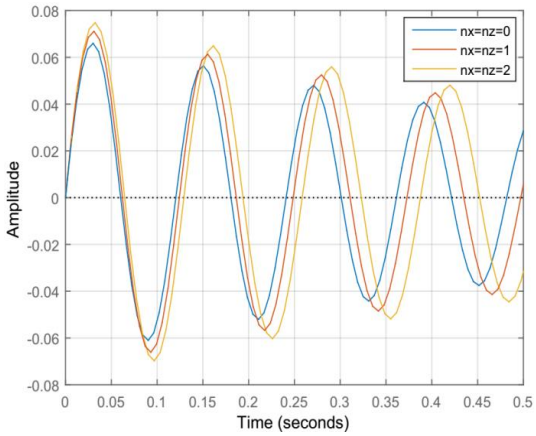

Figure 10. *Zoom Transient response of cantilever FGM variable value of law power index*

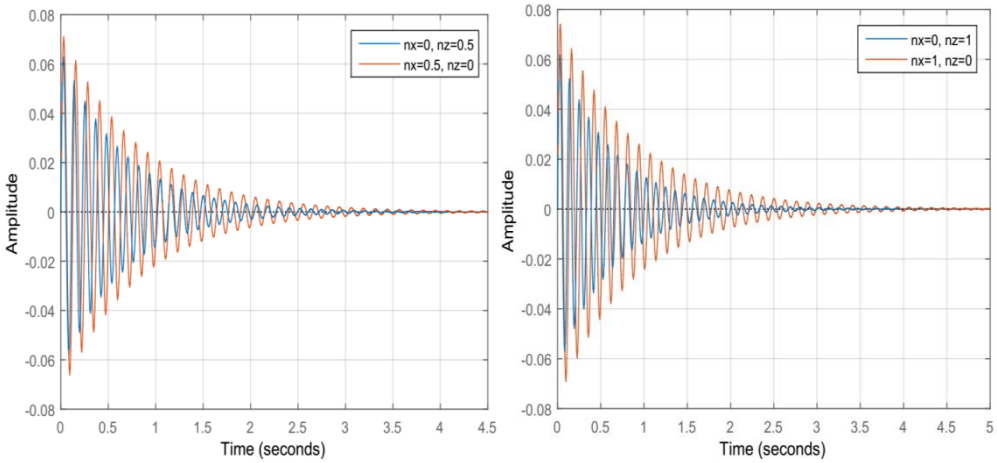

Figure 11. *Transient response of cantilever FGM beam with variable value of law power index*

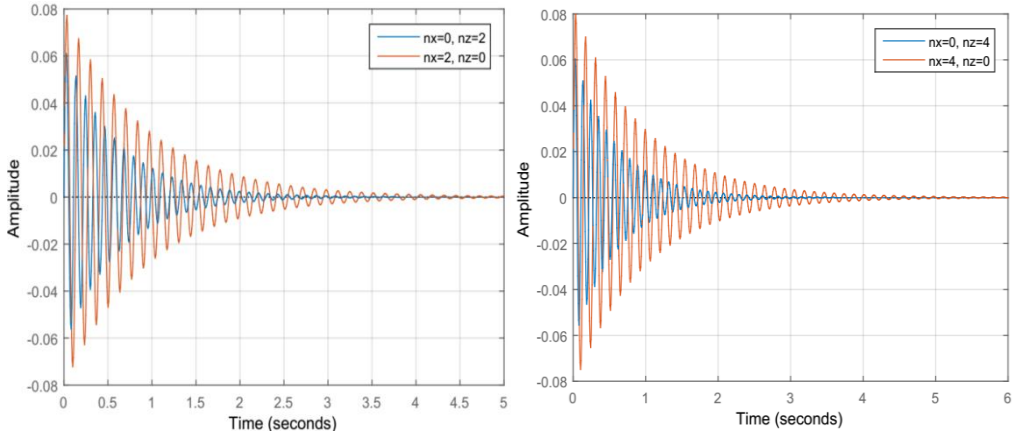

Figure 12. *Transient response of cantilever FGM beam with variable value of law power index*

Some of the above Figures are collected and put in one figure presenting the transient response for each direction of the FGM beam and presented in Figure 13 and Figure 14, where nz=0 and nx=0, respectively. The response of the FG beam in Figure. 14 (nz=0) is smaller than that corresponding in Figure 13 (nx=0). That means properties distribution in the axial (longitudinal) direction shows more effect on the dynamic characteristics of the cantilever FGM beam than their distribution in the transverse direction.

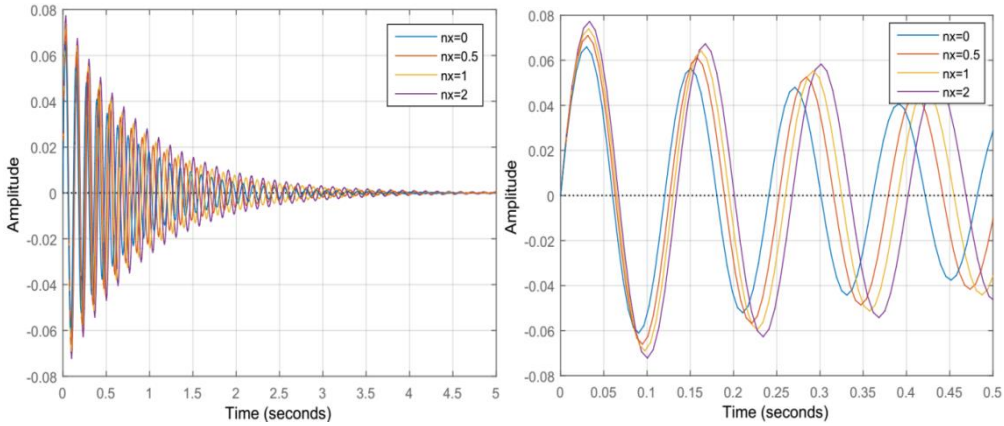

Figure 13. *a) Transient response of cantilever FGM beam with nz=0, b) Zoom of the transient response.*

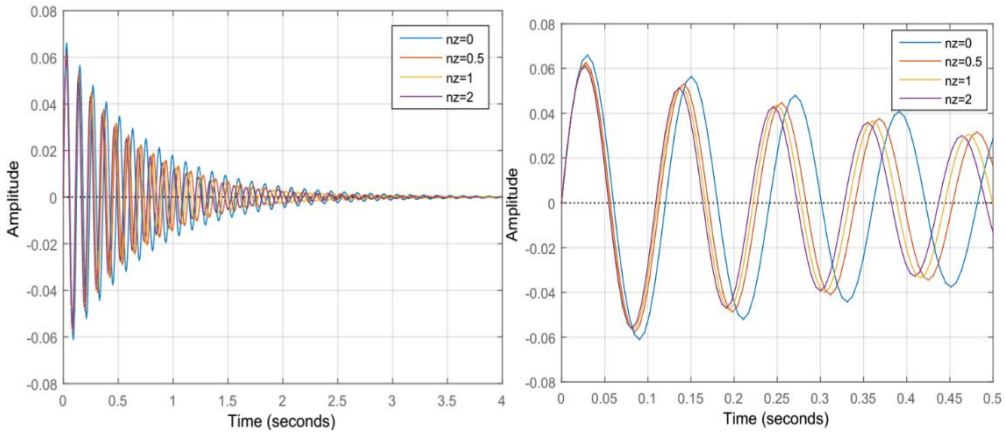

Figure 14. *a) Transient response of cantilever FGM beam with nx=0, b) Zoom of the transient response.*

3.5 Effect of Moduli on the Dynamic Characteristics

When the FGM is considered as only one material (nx=nz=0), the response of the beam decreases as the modulus ratio (E2/E1) increases (inverse relationship). The difference between the dynamic response increases as the difference in the module's ratios increases. The zoomed response shown in Figure 15b shows that the frequency increase as the ratio increase due to an increase the beam stiffness due to domination the material of the higher stiffness, which in turns increases the system

From a simple comparison between Figures 15-17, similar behavior can be noticed with increasing the power law index in both directions for the same reason mentioned above. However, the FGM beam shows higher dynamic response for all the values of the modulus ratio. That is because of the variations in the material properties distribution that produce beam with relatively lower stiffness. This conclusion is confirmed in the previous section due to the variation in the power law indexes. Furthermore, Figures 15b, Figure 16b, and Figure 17b show that the sensitivity of the transient response and the frequency to the increasing in the modules ratio decreases as the power low indexes increases.

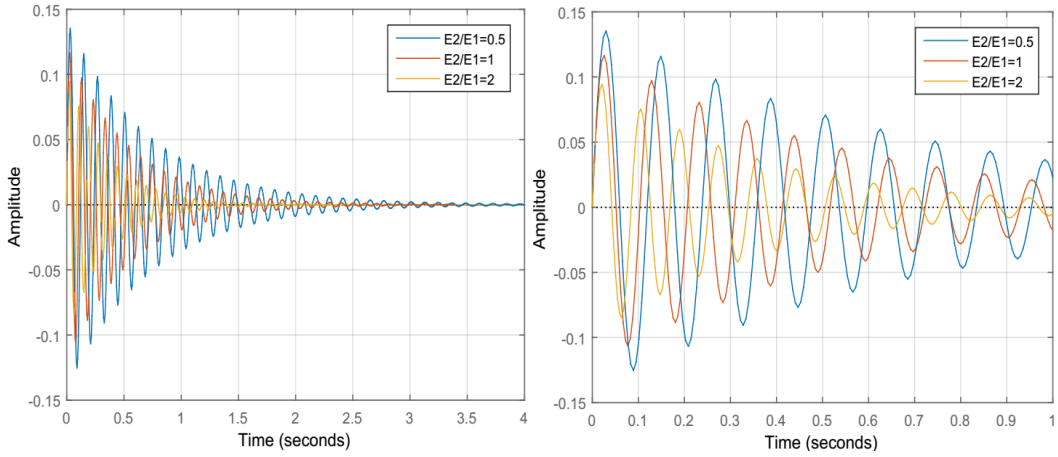

Figure 15. *a) Transient response of cantilever FGM beam with varying modulus ratio for nx=nz=0 b) Zoom of the transient response*

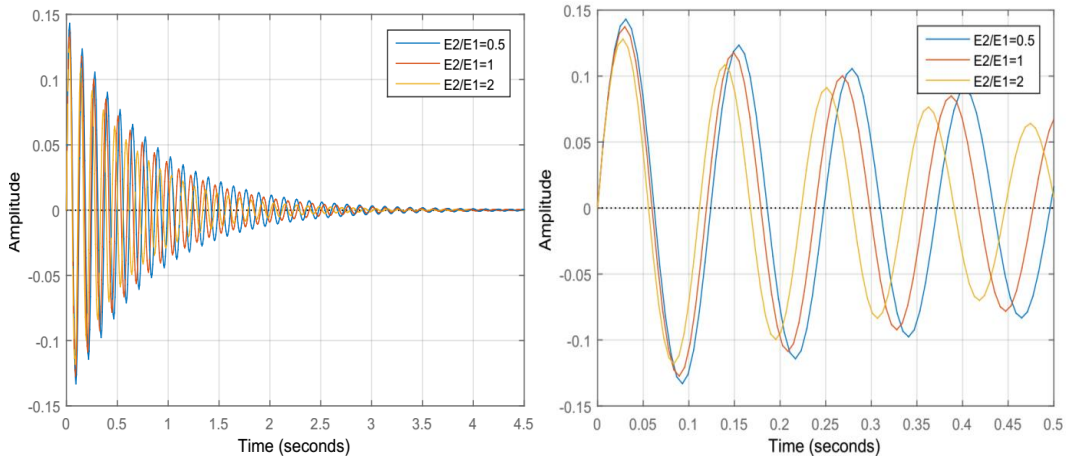

Figure 16. *a) Transient response of cantilever FGM beam with varying modulus ratio for nx=nz=1 b) Zoom of the transient response*

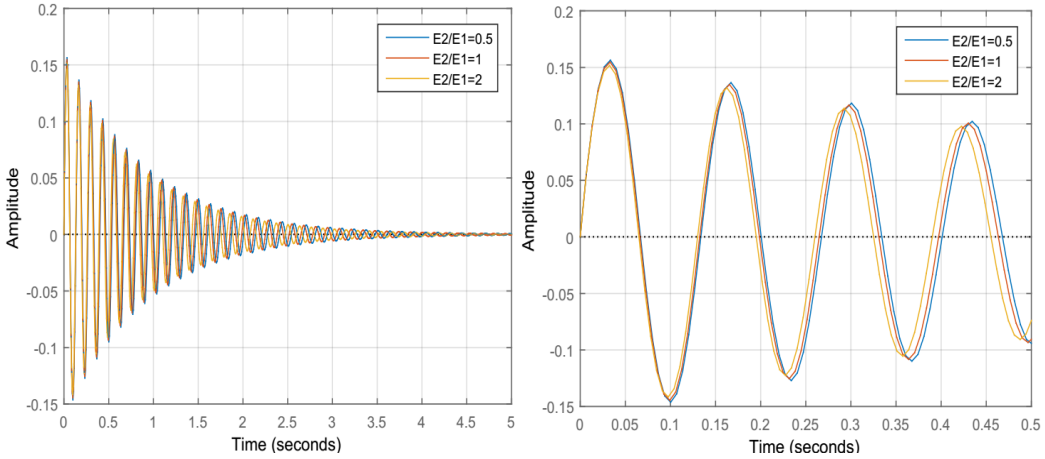

Figure 17. *a) Transient response of cantilever FGM beam with varying modulus ratio for nx=nz=4 b) Zoom of the transient response*

The response increases as the index nx increase. However, the differences decreases as the modules ratio and nz increases. The higher modulus ratio, the higher the frequency and smaller steady state time. Maximum displacement is noticed at the maximum PI and minimum of the modulus ratio as shown in Figures 18-20.

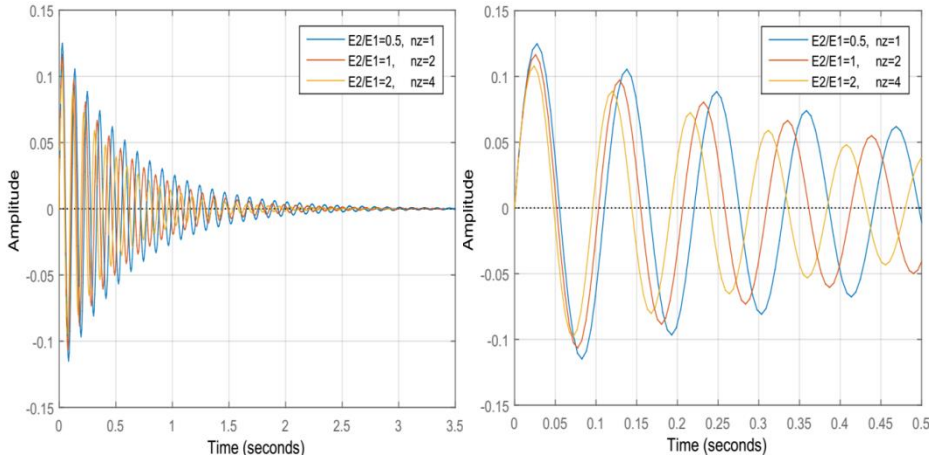

Figure 18. *a) Transient response of cantilever FGM beam with varying modulus ratio for nx=0 b) Zoom of the transient response*

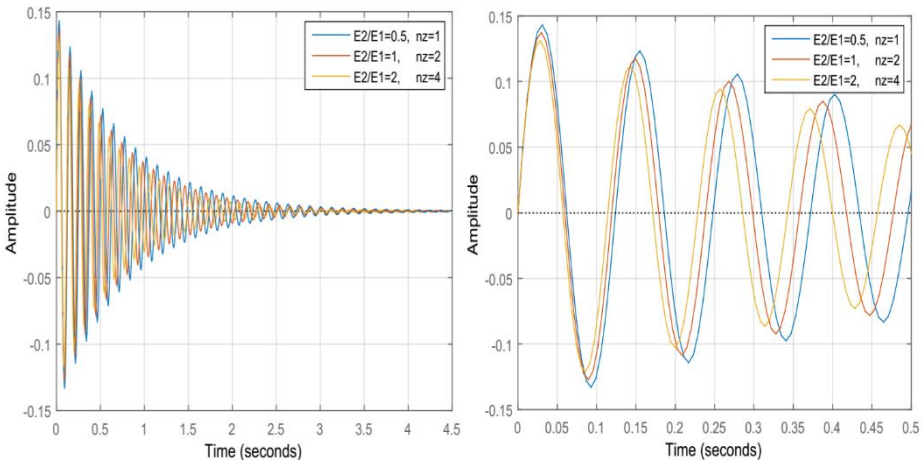

Figure 19. *a) Transient response of cantilever FGM beam with varying modulus ratio for nx=1 b) Zoom of the transient response*

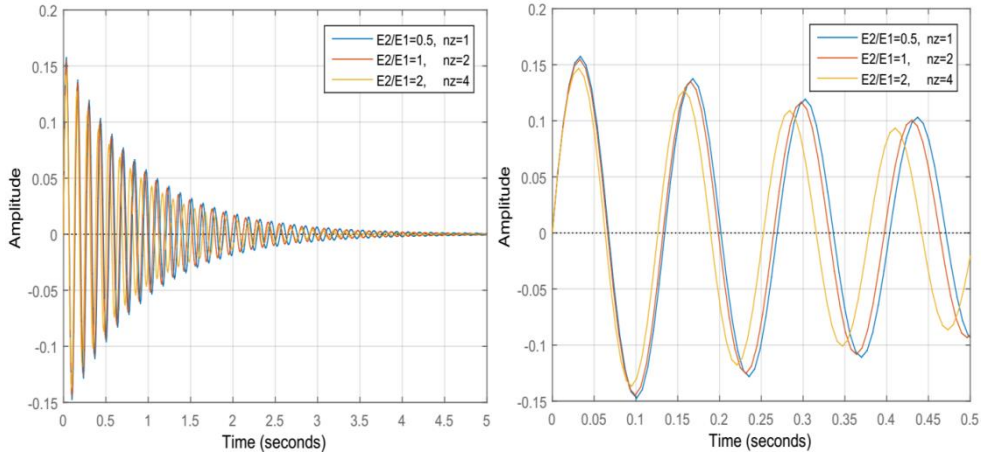

Figure 20. *a) Transient response of cantilever FGM beam with varying modulus ratio for nx=4 b) Zoom of the transient response*

4. CONCLUSION

Modal and transient analyses for FG Timoshenko beam, where the MP vary in two directions, are investigated in this work. The effect of PI on the mode shapes and the response are presented. Effect of modulus ratio is presented as well. For validation purposes. Some conclusions are emerged and can be illustrated as follows:

1. The FEM well predicted the natural frequency and the response of the FG beam.
2. The variations in the power law index in the longitudinal direction show more impact on the frequency of the beam than that corresponding in transverse direction.
3. The highest frequencies of the two-dimension FGM beam are obtained at lower values of the PI and higher values of the modulus ratios.
4. Material distribution in the longitudinal direction has more impact on the transient response than that corresponding in the transverse direction.
5. The sensitivity of the transient response and the frequency to the increasing in the module's ratio decreases as the PIs increases.
6. Maximum displacement is noticed at the maximum values of the PI and minimum value of the modulus ratio.
7. To enhance dynamic characteristics of a structural beam design, controlling the vibration of the 2D-FG beam can be achieved by choosing suitable PI and modulus ratios.

References

[1] Sankar, B. V. (2001). An elasticity solution for functionally graded beams. *Composites Science and Technology*, *61*(5), 689-696.

[2] Aubad, M. J., Khafaji, S. O. W., Hussein, M. T., & Al-Shujairi, M. A. (2019). Modal analysis and transient response of axially functionally graded (AFG) beam using finite element method. *Materials Research Express*, *6*(10), 1065g1064.

[3] Şimşek, M., & Al-Shujairi, M. (2017). Static, free and forced vibration of functionally graded (FG) sandwich beams excited by two successive moving harmonic loads. *Composites Part B: Engineering*, *108*, 18-34.

[4] Al-shujairi, M., & Mollamahmutoğlu, Ç. (2018). Dynamic stability of sandwich functionally graded micro-beam based on the nonlocal strain gradient theory with thermal effect. *Composite Structures*, *201*, 1018-1030.

[5] Khafaji, S. O. W., Al-Shujairi, M. A., & Aubad, M. J. (2020). Transient analysis of transversely functionally graded Timoshenko beam (TFGTB) in conjunction with finite element method. *Archive of Mechanical Engineering*, *67*.
[6] Karamanli, A. (2017). Static behaviour of two-directional functionally graded sandwich beams using various beam theories. *New Trends in Mathematical Sciences*, *5*(2), 112-147.
[7] Karamanlı, A. (2018). Free vibration analysis of two directional functionally graded beams using a third order shear deformation theory. *Composite Structures*, *189*, 127-136.
[8] Wang, Z.-h., Wang, X.-h., Xu, G.-d., Cheng, S., & Zeng, T. (2016). Free vibration of two-directional functionally graded beams. *Composite Structures*, *135*, 191-198.
[9] Şimşek, M. (2016). Buckling of Timoshenko beams composed of two-dimensional functionally graded material (2D-FGM) having different boundary conditions. *Composite Structures*, *149*, 304-314.
[10] Karamanlı, A., & Vo, T. P. (2018). Size dependent bending analysis of two directional functionally graded microbeams via a quasi-3D theory and finite element method. *Composites Part B: Engineering*, *144*, 171-183.
[11] Karamanlı, A. (2017). Elastostatic analysis of two-directional functionally graded beams using various beam theories and Symmetric Smoothed Particle Hydrodynamics method. *Composite Structures*, *160*, 653-669.
[12] Şimşek, M. (2015). Bi-directional functionally graded materials (BDFGMs) for free and forced vibration of Timoshenko beams with various boundary conditions. *Composite Structures*, *133*, 968-978.
[13] Yas, M., & Heshmati, M. (2012). Dynamic analysis of functionally graded nanocomposite beams reinforced by randomly oriented carbon nanotube under the action of moving load. *Applied Mathematical Modelling*, *36*(4), 1371-1394.
[14] Deng, H., & Cheng, W. (2016). Dynamic characteristics analysis of bi-directional functionally graded Timoshenko beams. *Composite Structures*, *141*, 253-263.
[15] Tang, Y., & Ding, Q. (2019). Nonlinear vibration analysis of a bi-directional functionally graded beam under hygro-thermal loads. *Composite Structures*, *225*, 111076.
[16] Karamanlı, A. (2017). Bending behaviour of two directional functionally graded sandwich beams by using a quasi-3d shear deformation theory. *Composite Structures*, *174*, 70-86.
[17] Nejad, M. Z., Hadi, A., & Rastgoo, A. (2016). Buckling analysis of arbitrary two-directional functionally graded Euler–Bernoulli nano-beams based on nonlocal elasticity theory. *International Journal of Engineering Science*, *103*, 1-10.
[18] Yang, T., Tang, Y., Li, Q., & Yang, X.-D. (2018). Nonlinear bending, buckling and vibration of bi-directional functionally graded nanobeams. *Composite Structures*, *204*, 313-319.
[19] Li, L., Li, X., & Hu, Y. (2018). Nonlinear bending of a two-dimensionally functionally graded beam. *Composite Structures*, *184*, 1049-1061.
[20] Nejad, M. Z., & Hadi, A. (2016). Non-local analysis of free vibration of bi-directional functionally graded Euler–Bernoulli nano-beams. *International Journal of Engineering Science*, *105*, 1-11.
[21] Su, H., Banerjee, J., & Cheung, C. (2013). Dynamic stiffness formulation and free vibration analysis of functionally graded beams. *Composite Structures*, *106*, 854-862.
[22] Lin, Y.-H. (1994). Vibration analysis of Timoshenko beams traversed by moving loads. *Journal of Marine Science and Technology*, *2*(1), 4.